The neural mechanisms of reliability weighted integration of shape information from vision and touch

Hannah B. Helbig [a,*], Marc O. Ernst [a], Emiliano Ricciardi [b], Pietro Pietrini [b], Axel Thielscher [a], Katja M. Mayer [a], Johannes Schultz [a], Uta Noppeney [a]

[a] Max Planck Institute for Biological Cybernetics, Tübingen, Germany
[b] Laboratory of Clinical Biochemistry and Molecular Biology, University of Pisa, Pisa, Italy

ARTICLE INFO

ABSTRACT

Behaviourally, humans have been shown to integrate multisensory information in a statistically-optimal fashion by averaging the individual unisensory estimates according to their relative reliabilities. This form of integration is optimal in that it yields the most reliable (i.e. least variable) multisensory percept. The present study investigates the neural mechanisms underlying integration of visual and tactile shape information at the macroscopic scale of the regional BOLD response. Observers discriminated the shapes of ellipses that were presented bimodally (visual–tactile) or visually alone. A 2×5 factorial design manipulated (i) the presence vs. absence of tactile shape information and (ii) the reliability of the visual shape information (five levels). We then investigated whether regional activations underlying tactile shape discrimination depended on the reliability of visual shape. Indeed, in primary somatosensory cortices (bilateral BA2) and the superior parietal lobe the responses to tactile shape input were increased when the reliability of visual shape information was reduced. Conversely, tactile inputs suppressed visual activations in the right posterior fusiform, when the visual signal was blurred and unreliable. Somatosensory and visual cortices may sustain integration of visual and tactile shape information either via direct connections from visual areas or top-down effects from higher order parietal areas.

© 2011 Published by Elsevier Inc.

Introduction

Objects and events are commonly perceived through multiple senses including vision, touch and audition. The human brain is thus challenged to integrate information from different sensory modalities into a coherent and reliable percept. At the behavioral level, humans have been shown to integrate multisensory information by averaging independent sensory estimates according to their reliabilities (= inverse of variance). For instance, in visual–haptic discrimination of object size, the integrated percept has been shown to change gradually from visually to haptically dominant when the reliability of the visual estimate was progressively reduced (Ernst and Banks, 2002). This form of integration, also referred to as Maximum Likelihood Estimation (MLE), is optimal in that it yields the most reliable multisensory percept, that is, the percept associated with the least variance (e.g., Alais and Burr, 2004; Ernst and Banks, 2002; Ernst and Bülthoff, 2004; Hillis et al., 2004; Knill and Saunders, 2003). However, the neural mechanisms underlying visual–tactile integration are currently unclear.

Neurophysiological and functional imaging studies in human and non-human primates have revealed multisensory interactions in a widespread neural system encompassing subcortical structures (Calvert et al., 2001; Wallace et al., 1996), putative unisensory cortices (Bonath et al., 2007; Ghazanfar et al., 2005; Kayser et al., 2007; Lakatos et al., 2007; Martuzzi et al., 2007; Molholm et al., 2004; Schroeder and Foxe, 2002; van Atteveldt et al., 2004) and higher-order association cortices (Barraclough et al., 2005; Beauchamp et al., 2004; Ghazanfar et al., 2008; Macaluso et al., 2003; Miller and D'Esposito, 2005; Nath and Beauchamp, 2011; Noesselt et al., 2007; Noppeney et al., 2008, 2010; Sadaghiani et al., 2009).

In the visual–haptic domain, the anterior intraparietal sulcus (aIPS; extending even into the postcentral and superior parietal sulcus; see e.g., Stilla and Sathian, 2008; Zhang et al., 2004) is thought to play a key role in visual–tactile integration (Amedi et al., 2001, 2002, 2005; Banati et al., 2000; Beauchamp et al., 2010; Calvert et al., 2001; Gentile et al., 2011; Grefkes et al., 2002; Hadjikhani and Roland, 1998; James et al., 2002; Saito et al., 2003; see also Avillac et al., 2007 for neurophysiological evidence in VIP in non-human primates). Furthermore, a subregion within the lateral occipital complex (LOC) that is generally implicated in visual object processing (Grill-Spector et al., 1999; Malach et al., 1995) was also activated by tactile stimuli (3D haptic perception: e.g., Amedi et al., 2001; Stilla and Sathian, 2008; Zhang et al., 2004; perception of less complex tactile and haptic stimuli: e.g., Kim and James, 2010; Prather et al., 2004; Stoesz et al., 2003). Evidence for a role of LOC and IPS in visual–tactile shape processing has been provided primarily by conjunction inferences that demonstrated regional responses independently for visual and tactile shape relative to non-shape

* Corresponding author at: Max Planck Institute for Biological Cybernetics, Spemannstr. 41, 72076 Tübingen, Germany.
E-mail address: helbig@tuebingen.mpg.de (H.B. Helbig).

information (i.e. conjunction analyses identify activations common to several inputs, Amedi et al., 2001, 2002; Hadjikhani and Roland, 1998; Pietrini et al., 2004). Yet, conjunction inferences are limited for two reasons: First, conjunction inferences are predicated on the assumption that a "multisensory" region is individually activated by both unisensory inputs. This renders them blind to integration processes where one unisensory (e.g., visual) input in itself does not elicit a significant regional response, but rather modulates the response elicited by another input (e.g., tactile). In fact, at the single neuron level, recent neurophysiological studies have demonstrated that these sorts of modulatory interactions seem to be a rather common phenomenon in both, higher level regions such as VIP and, in particular, in "traditionally unimodal regions" (e.g., Foxe and Schroeder, 2005; Ghazanfar and Schroeder, 2006; Kayser and Logothetis, 2007; Kayser et al., 2005, 2008; Lakatos et al., 2007). Second, given the low spatial resolution of fMRI, conjunction analyses cannot formally distinguish whether visual and tactile information interact within a common region or are processed in independent neuronal populations (Calvert et al., 2001; Noppeney, 2011). This issue was recently addressed in an fMRI study that showed crossmodal (visual–haptic) adaptation effects in both LOC and aIPS in an adaptation paradigm (Tal and Amedi, 2008). These crossmodal adaptation effects may suggest that visual and tactile input do not only converge within a brain region but are indeed integrated within those areas (i.e. processed within identical neuronal populations). Alternatively, interaction approaches can be employed in fMRI to demonstrate that the response to one sensory input depends on or is influenced by signals in another sensory modality. In this manuscript, we investigate multisensory integration from this wider perspective of multisensory interactions (i.e. non-linear response combinations).

The present human fMRI study aimed to characterize the neural mechanisms of visual–tactile shape integration at the macroscopic scale of regional BOLD signals. More specifically, we investigated whether regional activations elicited by visual–tactile shape discrimination reflect the differential contributions of vision and touch to the bimodal percept. To answer this question, we combined psychophysics and fMRI in a novel interaction approach that weights the interaction contrast (see Calvert et al., 2001; Noppeney, 2011) according to the reliabilities of the unimodal estimates, as measured in a prior psychophysics study (Helbig and Ernst, 2007a). This constrained interaction approach enables us to investigate whether activations elicited by tactile shape processing or the effect of tactile input on visual

processing are modulated by the reliability of visual shape input as predicted by the Maximum Likelihood Estimation model. In brief, we presented observers with visual or visual–tactile ellipses (see Fig. 1) while manipulating (i) the presence vs. absence of tactile shape information and (ii) the reliability of the visual shape information (modulated by a blur filter degrading the visual information at five levels, Vblur0, Vblur1, Vblur2, Vblur3, Vblur∞, ranging from clearly defined to completely blurred visual shape) in a 2×5 factorial design. First, we used behavioural measures to demonstrate that humans integrate visual and tactile shape information in a statistically-optimal fashion (even under adverse experimental conditions, with visual information presented via mirrors and hence spatially discrepant from the tactile input as in the scanner environment; see also Helbig and Ernst, 2007b). If visual and tactile information are indeed fused into a unified percept in a statistically-optimal fashion, the psychophysically measured variance (= inverse of reliability) of the integrated percept should be smaller than the variances of either individual sensory estimate. Second, we used fMRI to explore whether the BOLD response elicited by tactile shape processing is modulated by the reliability of the visual shape information (and vice versa). Given the ubiquity of multisensory integration processes within the neocortex of the primate brain (e.g., Foxe and Schroeder, 2005; Ghazanfar and Schroeder, 2006; Kayser and Logothetis, 2007; Kayser et al., 2005, 2008; Lakatos et al., 2007; Werner and Noppeney, 2010a, 2010b), we aimed to define the level within the cortical hierarchy (e.g. primary sensory vs. higher order association cortices) where BOLD responses to and effects of tactile shape input are modulated by the reliability of visual shape information by testing for the positive and negative interactions between tactile input and visual reliability. Specifically, we hypothesized that areas involved in tactile processing (e.g. primary and secondary somatosensory cortex) show an activation enhancement for visuotactile relative to visual processing (i.e. VT+ to VT−) that grows with the weight given to the tactile signal during visuotactile integration (i.e. increases for low visual reliability). Conversely, we expected that visual shape processing areas (e.g. lateral occipital complex, LOC) show an activation enhancement for visuotactile relative to visual only processing (i.e. VT+ to VT−) that decreases with the weight for the tactile input (and hence increases with the visual weight and visual reliability). In fact, adding tactile information to unreliable and fully blurred visual input may even suppress activation in shape processing areas resulting in an activation decrease for visuotactile relative to
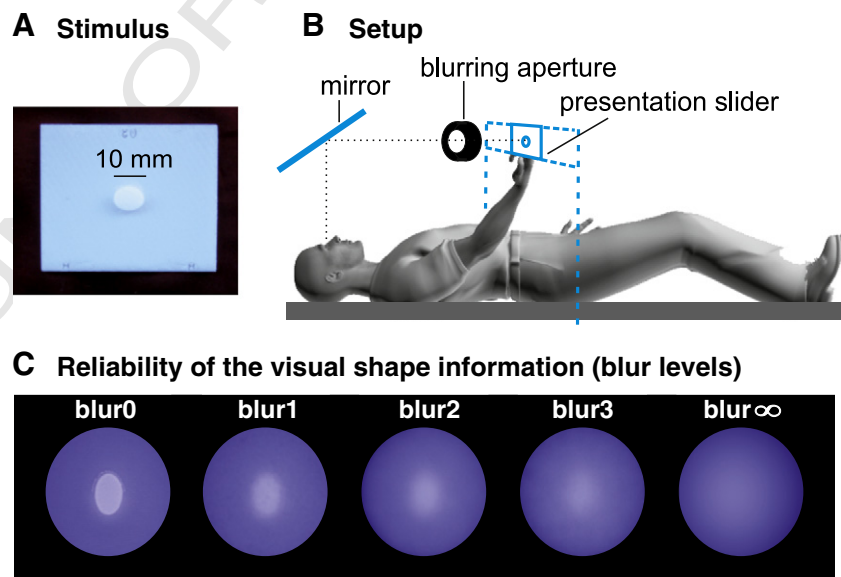
Fig. 1. Stimuli and paradigm. A: Example of a visual–tactile stimulus. B: Participants viewed the ellipse on the front side of the panel (visual stimulus) and touched the elliptic ridge on the back side (tactile stimulus). C: Photographs of the visual stimuli viewed through a blurring aperture: The visual shape information was progressively degraded by applying five levels of blur ranging from Vblur0 (intact visual shape) to Vblur∞ (visual shape information absent).

visual only processing. In sum, we expected both visual and somatosensory areas to exhibit interactions between visual reliability and tactile input, yet these interactions should emerge in opposite directions.

Methods

Participants

Twelve right-handed healthy volunteers (3 females; mean age: 25.1 years, range 22–31 years) with normal or corrected-to-normal vision and no history of neurological or psychiatric diseases gave informed consent to participate in the study. Due to a technical failure of stimulus–response recording, the behavioural data of one volunteer is not included in the behavioural analysis. The study was approved of by the joint human research review committee of the University of Tübingen and the Max Planck Society.

Stimuli and apparatus

The tactile stimuli were elliptic ridges (thickness 2.0 mm) of different length-to-width ratios mounted onto a planar plastic panel of 58.0 mm by 50.0 mm. The major axis of the ellipse was set to 10.0 mm and oriented either vertically (ver) or horizontally (hor). The minor axis was set to 8.0 or 8.8 mm. They were printed in 3D (Dimension 3D Printer, Stratasys®, Inc.), layer-by-layer, by depositing filaments of heated plastic (Acrylnitril–Butadien–Styrol). The printed objects were hard, white and opaque (see Fig. 1A).

For the visual–tactile conditions (VT+), two aligned ellipses of equal length-to-width ratios were mounted onto both sides of the panel to simulate a composite cylinder (with elliptical cross-section) protruding through the panel. Participants could see the ellipse on the front side of the panel via mirrors and reached out of the short bore of the head-scanner to touch the elliptic ridge on the back of the panel (see Fig. 1B). Visual and tactile ellipses were therefore always congruent in terms of diameter in the visual–tactile conditions. The visual stimuli subtended approximately 0.64 ° (max. extension 10.0 mm at a viewing distance of about 90 cm) at different blur levels.

For visual-only conditions (tactile shape information absent, VT−), participants were presented with only one ellipse attached to the front side of the panel, while the back side was blank. In the fixation condition (fix), both sides of the panel were flat, yet a black fixation dot (diameter 5.0 mm) was presented on the front side.

Experimental design

fMRI study

In a two-alternative forced-choice discrimination paradigm, subjects were presented with visual only (VT−) or visual–tactile (VT+) ellipses. Subjects fixated the ellipse on the front side of the panel and pressed with the finger tip of their right index finger against the back side of the panel that could either hold a congruent elliptical ridge or be blank. Thus, the shape of the ellipse needed to be extracted from the indentation of the fingertip rather than active exploratory movements. Subjects decided whether the major (i.e. longer) axis of the ellipse was oriented horizontally or vertically. They were trained to fixate the stimulus or fixation spot during the trials and discriminate the tactile shape without exploratory hand movements.

The 2×5 factorial design manipulated the visual and tactile inputs that defined the shape of the ellipse: (1) *Tactile Shape Information* was either present, T+, or absent, T−. (2) The reliability of the *Visual Shape Information* was manipulated with the help of blurring techniques (Helbig and Ernst, 2007a) to degrade visual shape information by five different degrees from V_{blur0} (= clearly defined), V_{blur1}, V_{blur2}, V_{blur3}, to $V_{blur\infty}$ (= fully blurred vision as indicated by chance performance, i.e. visual shape information was absent) (see Fig. 1C). In other words, tactile and visual inputs were given in all trials to control for low level multisensory integration effects (e.g., non-specific alertness effects). Yet, our experimental design manipulated the availability of shape information within the tactile (presence vs. absence) and visual (5 levels of blur) modalities. In addition, as a low level control condition, fixation trials (fix) were included where subjects fixated a dot and pressed their finger tip against a blank plane.

The beginning of each trial was indicated by a brief auditory signal (396 Hz, 100 ms). Concurrently, the stimuli were manually inserted into a presentation device by the experimenter (for further details see Helbig and Ernst, 2007a). After 3000 ms, a second auditory signal (220 Hz, 100 ms) indicated the beginning of the response interval of 1000 ms, in which participants responded by pressing one of two buttons with either the index or middle finger of the left hand (button assignment counterbalanced across participants) and the stimulus was manually replaced. In the fixation trials, subjects responded by pressing a pre-defined button. Stimuli were presented with a stimulus onset asynchrony of 4 s (= 3 s stimulus duration + 1 s inter-stimulus interval). Trials were presented in a mixed design: The factor Visual Shape Information was blocked in separate sessions, as the replacement of the "blur lens" could not be accomplished within the inter-stimulus-interval of 1000 ms. The factor Tactile Shape Information was randomized. Each session encompassed 20 tactile-present and 20 tactile-absent trials of one particular blur level. Within a session, each of the four different ellipses (i.e. horizontal length 8.0 mm or 8.8 mm, vertical length: 8.8 mm or 8.0 mm) was presented 10 times (once in each condition). In all trials, visual and tactile ellipses were identical, i.e. the fMRI study included only congruent, no-conflict trials. There were 40 trials for each visual shape information condition (V_{blur0}, V_{blur1}, V_{blur2}, V_{blur3}, $V_{blur\infty}$). Each of the 5 blocks was repeated twice (i.e., a total 400 trials). The order of blocks was randomized and counter-balanced within and across subjects. The V_{blur0} and $V_{blur\infty}$ sessions included ten additional blocks of five fixation trials.

Psychophysics study (outside the scanner)

A subset of six participants also participated in a prior psychophysics study outside the scanner environment, but with the identical experimental set-up, elliptical stimuli and task (for full details, see Helbig and Ernst, 2007a). In contrast to the fMRI experiment, the visual–tactile conditions included both, non-conflict and conflict trials. Conflict-trials introduced a small conflict between tactile and visual ellipses that was not noticed by the participants. These conflict trials enabled us to evaluate, whether the visual and tactile weights for the different blur levels were indeed determined as predicted by Maximum Likelihood Estimation (see below).

Computation of sensory reliabilities based on behavioural responses from psychophysics (outside the scanner) and fMRI study (inside the scanner)

The reliabilities of the tactile and visual unimodal estimates at each blur level can be computed from the just noticeable differences (JND) of the unimodal psychometric functions (psychophysics; Helbig and Ernst, 2007a; Ernst and Banks, 2002) and also from the unimodal d-primes (fMRI; Treisman, 1998). From these unimodal sensory estimates of reliability (= inverse of variance), the following two parameter-free key predictions can be derived according to statistically optimal integration (Maximum Likelihood Estimation). First, the variance of the bimodal visual–tactile estimate should be smaller than the variance of either unimodal estimate. Second, the unimodal estimates should be weighted according to their unimodal reliabilities in the combined estimate. The first prediction can be evaluated using the congruent non-conflict trials that were presented in both psychophysics and fMRI study. The second prediction is evaluated based on the conflict trials that were presented only in the psychophysics study.

Briefly, in the psychophysics study (outside the scanner), psychometric functions (cumulative Gaussians) were fitted separately to the data of the unimodal and bimodal conditions at each blur level. The reliabilities of the tactile and visual unimodal estimates at each blur level were computed based on the just noticeable differences (JND) of the unimodal psychometric functions. Indeed, the psychophysics experiment confirmed both predictions. As predicted by statistically optimal integration, the variance (as indexed by the JND) of the visual–tactile estimate was reduced by the predicted amount relative to both unimodal estimates. Further, the conflict trials showed that the contributions of the visual and tactile inputs to the bimodal percepts were weighted according to the relative unimodal reliabilities. In particular, following the predictions of statistically optimal integration the influence of the tactile input on the bimodal percept increased with decreasing visual reliability as a result of visual blurring.

Importantly, the psychophysics study included 3264 trials per subject leading to precise estimates of subjects' sensory reliabilities based on the JND of the psychometric function. Furthermore, the inclusion of conflict trials allowed us to formally evaluate whether indeed subjects integrated the visual and tactile shape information weighted according to the reliabilities of the unisensory estimates.

In contrast, inside the fMRI study, only two different types of ellipsoids were presented, so that no psychometric functions could be derived. Nevertheless, assuming the equal variance Gaussian model, the sensory reliabilities can be computed from d-primes that basically represent the difference between vertical and horizontal ellipsoids in units of standard deviation (i.e. (Mean_vertical − Mean_horizontal)/sqrt (variance)). Since the difference between vertical and horizontal ellipsoids (i.e. the ratio of the major and minor axes) is held constant over different levels of visual reliability, differences in d prime represent differences in signal reliability. Hence, the d primes can be used as an index of sensory reliability to compute the sensory weights (Treisman, 1998). However, the computation of sensory reliability from d prime is far less precise than from a psychometric function. Further, the fMRI study included only 40 trials per condition amounting to 400 trials per subject. Finally, the fMRI study included only congruent trials, but no conflict trials. These considerations motivated us to use the sensory weights estimated from the prior psychophysics study in the fMRI analysis rather than the weights that were estimated based on the d-primes from the fMRI study. However, the across-subjects sensory weights from the psychophysics and the fMRI study were in fact highly correlated with a correlation coefficient of 0.98 over conditions. This high correlation suggests that the profile of sensory weights is actually comparable across the fMRI and the psychophysics study indicating that both approaches would provide us with nearly equivalent activation results.

Image acquisition

A 3T Siemens Allegra system was used to acquire both T1 anatomical volume images ($1 \times 1 \times 1$ mm^3 voxels) and T2*-weighted echoplanar images with blood oxygenation level-dependent (BOLD) contrast (GE-EPI, Cartesian k-space sampling, TE = 39 ms, flip angle 90, TR = 2.61 s, 38 axial slices, acquired sequentially in descending direction, matrix 64×64, spatial resolution $3 \times 3 \times 3$ mm^3 voxels, interslice gap 0.6 mm, slice thickness 2.4 mm). There were ten sessions with a total of 76 or 137 (137 for V_{blur0} and $V_{blur\infty}$) volume images per session. The first six volumes were discarded to allow for T1 equilibration effects.

fMRI data analysis

The data were analyzed with statistical parametric mapping (using SPM2 software from the Wellcome Department of Imaging Neuroscience, London; http//www. fil.ion.ucl.ac.uk/spm, Friston et al., 1999). Scans from each subject were realigned using the first as a reference, spatially normalized into MNI standard space (Evans et al., 1992) resampled to $3 \times 3 \times 3$ mm^3 voxels and spatially smoothed with a Gaussian kernel of 6 mm full width at half maximum (FWHM). The time series in each voxel was high-pass filtered to 1/128 Hz. An AR1 + white noise model was used to accommodate serial autocorrelations. The fMRI experiment was modeled in an event related fashion using regressors obtained by convolving each event related unit impulse with a canonical hemodynamic response function and its first temporal derivative. We modeled the fixation and the 10 activation conditions in our 5×2 factorial design. Nuisance covariates included the realignment parameters (to account for residual motion artifacts). Condition-specific effects for each subject were estimated according to the general linear model and passed to a second-level analysis as contrasts. This involved creating the following contrast images for each subject at the first level:

Visual shape processing: $(V_{blur0}T-) - (V_{blur\infty}T-)$

Visual shape processing was identified by comparing $V_{blur0}T-$ to $V_{blur\infty}T-$, i.e. visual shape present (in the absence of tactile shape) relative to visual shape information absent (in the absence of tactile shape). However, since these two conditions could not be included in the same session for technical reasons (see Experimental design), we used an indirect approach. To allow for a comparison across separate scanning sessions, we first compared $V_{blur0}T-$ and $V_{blur\infty}T-$ individually with fixation baseline condition (within each session). The two resulting contrast images were then compared with each other $[(V_{blur0}T- \text{ to fix}) - (V_{blur\infty}T- \text{ to fix})]$.

Tactile shape processing: $(V_{blur\infty}T+) - (V_{blur\infty}T-)$

To identify tactile shape processing areas, we compared the tactile shape processing condition $V_{blur\infty}T+$ (i.e. tactile shape information in the absence of visual shape information) to the condition $V_{blur\infty}T-$ (i.e. absent tactile shape information, in the absence of visual shape information).

Visual–tactile interaction: $w_0 (V_{blur0}T+-V_{blur0}T-) + w_1 (V_{blur1}T+-V_{blur1}T-) + w_2 (V_{blur2}T+-V_{blur2}T-) + w_3 (V_{blur3}T+-V_{blur3}T-) + w_\infty (V_{blur\infty}T+-V_{blur\infty}T-)$

This interaction contrast identifies responses to tactile input that depended non-linearly on the reliability (level of blur) of the visual input as predicted by statistically optimal integration. A significant interaction reflects the differential contribution of vision and touch to the bimodal response at multiple visual blur levels. It indicates that the amount of visual blurring (reduced reliability of the visual input) modulates the response to tactile shape input. Generally, an interaction contrast is defined as a difference in differences. In the most simple 2×2 interaction, it reduces to w_0 $(V_{blur0}T+-V_{blur0}T-) + w_1 (V_{blur1}T+-V_{blur1}T-)$ with $w_0 = 1$ and $w_1 = -1$. Yet, our design included 5 levels of visual reliability as a parametric factor. Conventionally, interactions between a categorical factor (i.e. tactile shape present vs. absent) and a parametric factor (i.e. 5 levels of visual blur) are evaluated by assuming linear weighting (i.e. $w_0 = 2$, $w_1 = 1$, $w_2 = 0$, $w_3 = -1$, $w_\infty = -2$). In this study, we used a more refined approach and set the contrast weights wi to the mean corrected relative tactile cue weights as measured in a prior psychophysical experiment (see Helbig and Ernst, 2007a, tactile weights: blur0: $w_T = 0.2$, blur1: $w_T = 0.23$; blur2: $w_T = 0.56$; blur3: $w_T = 0.74$; blur∞: $w_T = 1.00$; mean corrected tactile weights: blur0: $w_0 = -0.347$, blur1: $w_1 = -0.3192$; blur2: $w_2 = 0.0115$; blur3: $w_3 = 0.1992$; blur∞: $w_\infty = 0.4554$). Applying sensory weights to the difference $VT - V$ rather than directly to V enables us to control for changes in visual input per se (because they cancel in the simple difference) and focus selectively on the effect that visual reliability exerts on tactile processing.

Please note that the across subjects' tactile cue weights from the prior psychophysics study (i.e. derived from the JND of the psychometric function) and the fMRI study (i.e. derived from d-primes) were highly correlated with a correlation coefficient of 0.98 indicating that identical results would have been obtained using the cue weights from the psychophysics study.

In addition to these specific contrast images, we also created contrast images comparing VT and V conditions separately at each level of visual reliability. All contrast images were spatially smoothed with a Gaussian kernel of 8 mm FWHM and entered into separate second level one-sample t-tests or an ANOVA (VT − T contrasts) to enable an unconstrained F-contrast (see below). Inferences were made at the second level to allow for a random effects analysis and generalization to the population (Friston et al., 1999).

Search volume constraints

All contrasts were tested for within (i) the entire brain and (ii) the LOC (LO and posterior fusiform pFUS). The search volume in the LOC was constrained to spheres of radius 10 mm centered on the coordinates −39, −78, −3 (left LO), +42, −75, −6 (right LO), −39, −57, −15 (left pFUS) and 39, −57, −15 (right pFUS; from Vinberg and Grill-Spector, 2008).

Unless otherwise stated, we report activations at p<0.05 corrected for multiple comparisons at the cluster level within the entire brain using an auxiliary uncorrected voxel threshold of p<0.001 (i.e. the correction is applied for spatial extent of clusters when the SPMs are thresholded at p<0.001 uncorrected). Because of the greater spatial precision, the region of interest analyses were corrected at the voxel level for multiple comparisons within our search volume of interest (i.e. LO and pFus).

Results

In the following, we report (1) the behavioural results and (2) the functional imaging results pertaining to the main effects of visual and tactile shape processing and the interaction between visual and tactile shape information.

Behavioural results (during fMRI experiment)

A two-way, repeated measurement ANOVA of performance accuracy with factors Tactile Shape Information (T+, T−) and Visual Shape Information (V_{blur0}, V_{blur1}, V_{blur2}, V_{blur3}, $V_{blur\infty}$) identified significant main effects of Tactile Shape Information ($F(1,10) = 34.67$, $p<.001$, sphericity assumed), Visual Shape Information ($F(4, 40) = 68.89$, $p<.001$ sphericity assumed) and a significant interaction between the two ($F(4, 40) = 15.84$, $p<.001$, sphericity assumed) (see Fig. 2). The improvement in performance for bimodal (V T+) relative to unimodal visual (V T−) input is more pronounced for degraded visual input (see Fig. 2). For blur levels 2 and 3 (one-tailed paired-sample t test: blur2: p<.012 blur2: p<.001), higher accuracies were observed for the visual–tactile estimate relative to both the visual and the tactile estimates (n.b. in a 2-AFC task, accuracy is related to d-prime and hence reliability of the sensory estimates). In a qualitative sense, this finding is consistent with the principle of statistically optimal integration, whereby the reliability of the visual–tactile estimate is greater than the reliability of either unimodal estimate. For blur levels 0 and 1, an increase in performance accuracy could not be observed because of ceiling effects (one-tailed paired-sample t test: blur0: p>.34, blur1: p>.20), which is in line with the results of our previous psychophysics study. In conclusion, the increase in reliability for the visual–tactile relative to the visual or tactile shape estimates suggests that subjects integrated visual and tactile shape information qualitatively in line with the principles of statistically optimal integration. Given the limited number of trials that did not provide precise estimates of subject-specific reliabilities, we refrained

behavioral data
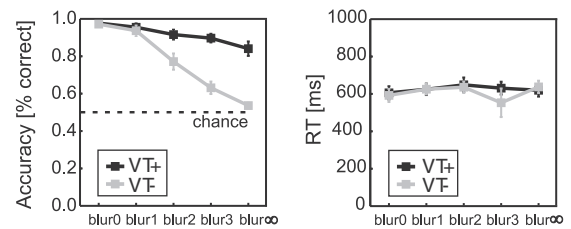
Fig. 2. Behavioural data. Accuracy is shown as a function of the reliability of the visual shape information (Vblur0, Vblur1, Vblur2, Vblur3, Vblur∞). Black denotes conditions where visual and tactile shape information were presented; gray denotes conditions where tactile shape information was absent, i.e., shape information was presented only in the visual modality.

from additional quantitative analyses to truly confirm statistically optimal integration.

For reaction times (limited to correct trials only), a two-way repeated measurement ANOVA did not reveal any significant main effects of Tactile Shape Information ($F(1; 10) = 1.59$, $p = .24$, sphericity assumed), Visual Shape Information ($F(4; 40) = 1.12$, $p = .36$, sphericity assumed) or an interaction between the two ($F(4; 40) = 1.47$, $p = .23$, sphericity assumed). Behavioural effects may be reflected primarily in terms of accuracy, since the task instructions emphasized accuracy rather than speed.

Behavioural results (outside the scanner, prior to fMRI experiment)

Our previous psychophysics study using stimuli and task that were identical to our fMRI experiment demonstrated that visual and tactile shape information is integrated in a statistically-optimal fashion i.e. weighted according to their unimodal reliabilities (for further details see Helbig and Ernst, 2007a). Furthermore, additional conflict trials confirmed that the tactile weights increased when the visual shape information was rendered unreliable by different amounts of visual blurring.

Functional imaging results

The functional imaging analysis was performed in two steps: First, we identified the neural systems underlying visual and tactile shape processing. Second, we identified regions that showed a significant interaction between visual and tactile shape processing (separately for positive and negative interactions).

Visual shape processing: $(V_{blur0}T-) - (V_{blur\infty}T-)$

Intact visual shape relative to absent visual shape significantly increased activations within the left occipital-temporal cortex (x, y, z coordinates: −42, −60, −24; z = 3.75, p = 0.015 corrected for multiple comparisons within pFUS) that has previously been implicated in visual shape processing (Grill-Spector et al., 1999; Malach et al., 1995).

Tactile shape processing: $(V_{blur\infty}T+) - (V_{blur\infty}T-)$

Tactile shape processing relative to touching a plane panel (i.e. tactile shape absent) enhanced activation in an extensive distributed system encompassing the postcentral sulci/gyri and superior parietal gyri bilaterally extending into the anterior intraparietal sulcus, the right inferior parietal gyrus, the right cerebellum, the right inferior frontal sulcus and the pre-supplementary motor area/cingulate sulcus (see Table 1). Brain activation in the bilateral postcentral sulcus is close to areas that have previously been shown to be involved in tactile orientation classification (Kitada et al., 2006; Van Boven et al., 2005). Comparing processing of T+ (tactile input present) versus T− (no tactile input) also elicited **Q6**

Table 1

Anatomical region	Side	Coordinates			p-value	z-value	Number of voxels
		x	y	z			
Visual shape processing							
Lateral occipital complex (pFUS)	L	−42	−60	−24	0.015	3.76	−[a]
Tactile shape processing							
Postcentral sulcus/gyrus (area 2)	R	54	−27	48	<0.001	4.68	328
Postcentral sulcus (area 2)	R	45	−36	51		4.13	
Inferior parietal gyrus	R	66	−15	15		4.21	
Postcentral sulcus/gyrus (area 2)	L	−51	−36	54	<0.001	4.58	515
Postcentral sulcus/gyrus (area 2)	L	−54	−33	45		4.55	
Superior parietal gyrus	L	−36	−54	63		4.93	
Cerebellum	R	15	−63	−21	0.004	4.36	53
Cerebellum	R	18	−57	−27		4.23	
Precentral gyrus	L	−42	−6	57	0.005	4.18	50
Precentral gyrus	L	−24	−9	69		3.95	
Precentral gyrus	L	−36	−9	63		3.72	
Pre-supplementary motor area	L	−3	3	54	<0.001	4.15	81
Cingulate sulcus	L	−6	15	39		4.06	
Inferior frontal sulcus	R	60	12	27	0.024	3.98	378
Inferior frontal sulcus	R	63	12	15		3.77	
Inferior sulcus/superior parietal gyrus	R	30	−57	63	<0.001	3.76	63
Inferior sulcus/superior parietal gyrus	R	21	−66	60		3.70	
Inferior sulcus/superior parietal gyrus	R	27	−48	69		3.61	
Visual-tactile shape interaction (positive)							
Postcentral sulcus/gyrus (area 2)	L	−51	−36	54	<0.001	4.98	170
Superior parietal gyrus	L	−36	−54	63		4.07	
Postcentral sulcus/gyrus (area 2)	R	54	−27	48	0.030	4.10	38
Visual-tactile shape interaction (negative)							
Lateral occipital complex (pFUS)	R	33	−63	−18	0.01	3.86	−[a]

Q2   [a] Small volume corrected (see Methods).

activation in areas of the motor system, most likely because pressing a finger against an ellipse and a blank pane involve slightly different motor patterns.

Positive visual–tactile interaction: $w_0 (V_{blur0}T+ - V_{blur0}T-) + w_1 (V_{blur1}T+ - V_{blur1}T-) + w_2 (V_{blur2}T+ - V_{blur2}T-) + w_3 (V_{blur3}T+ - V_{blur3}T-) + w_\infty (V_{blur\infty}T+ - V_{blur\infty}T-)$

To identify where and how tactile shape processing is modulated by visual shape information, we tested for the visual–tactile interaction. Generally, an interaction is a difference in differences (e.g. $V_{blur(i)}T+ - V_{blur(i)}T-$). For each level of visual reliability (V_{blur0}, V_{blur1}, V_{blur2}, V_{blur3}, $V_{blur\infty}$) we computed the contrast ($V_{blur(i)}T+ - V_{blur(i)}T-$). In brain areas where visual and tactile input is processed independently, the difference in activation should be constant across blur levels and simply reflect "tactile processing" (under the assumption of additivity, the effect (or weight) of the tactile component will be identical across all visual blur levels). In brain areas where visual shape information modulates and interacts with tactile shape input, the effect of the tactile shape input—as indexed by the contrast ($V_{blur(i)}T+ - V_{blur(i)}T-$)—will depend on the visual blur level. In other words, the difference ($V_{blur(i)}T+ - V_{blur(i)}T-$) pertaining to tactile shape processing depends on the blur level. This interaction can be formally described by assigning unequal weights to the $V_{blur(i)}T+ - V_{blur(i)}T-$ contrasts. We constrained the interaction contrast by using the tactile cue weights measured in a previous psychophysical experiment with identical task and stimuli (Helbig and Ernst, 2007a) (mean corrected tactile weights: blur0: $w_0 = -0.347$, blur1: $w_1 = -0.3192$; blur2: $w_2 = 0.0115$; blur3: $w_3 = 0.1992$; blur∞: $w_\infty = 0.4554$; n.b. after mean correction, some weights turn negative, so that they sum to zero). This positive interaction contrast reveals somatosensory or tactile processing areas, where the activation difference ($VT+ - VT-$) grows with increasing blur levels. It indicates that the amount of visual blurring (reduced reliability of the visual input) modulates the response to tactile shape input.

A significant visual–tactile interaction was revealed within somatosensory areas including the left and right postcentral sulci/gyri and the left superior parietal gyrus (see Table 1 and Fig. 3). As shown in Fig. 4, contrast estimates pertaining to the effect of tactile shape information ($V_{blur(i)}T+ - V_{blur(i)}T-$) at peak voxels (54, −27, 48 and −51, −36, 54) increase with reduced reliability of the visual shape information (V_{blur0}, V_{blur1}, V_{blur2}, V_{blur3}, $V_{blur\infty}$) in line with the tactile weights (serves illustrative purposes).

On the basis of probabilistic cytoarchitectonic maps (Eickhoff et al., 2005) the peak activations in the left (−51, −36, 54; z=4.98) and right (54, −27, 48; z=4.10) postcentral sulci/gyri can be assigned to area 2 with a probability of 70% and to area 1 with a probability of 30%. The activation maxima of the left superior parietal lobe (−36, −54, 63; z=4.07) can be assigned to area 2 with a probability of 20% (see Fig. 3B). As the shape discrimination task could be performed by identifying the orientation of the ellipse' major axis, not surprisingly, these areas are close to activations previously reported in tactile grating orientation judgments (Kitada et al., 2006; van Boven et al., 2005). In addition, a nonsignificant trend was found in the pre-supplementary motor area (3, 6, 54; z=3.79) and in the left thalamus (−18, −9, 0; z=4.36).

For in-depth characterization of our data, we have also employed a multidimensional F-contrast to investigate whether the difference between VT and T processing depends on the level of visual reliability without imposing a specific profile. This F-contrast revealed again the left (x = −51 y = −33 z = 42; z-score = 4.6; p = 0.09 corrected) and right (x = 57 y = −24 z = 48; z-score = 4.5; p = 0.17 corrected) postcentral sulcus/gyrus as the two regions with the most reliable activations in this statistical comparison. However, in this less constrained comparison, the activations were not significant when correcting for multiple comparisons. The less significant results in the somatosensory cortex are not surprising, since this F-contrast tests a less constrained hypothesis.

Negative visual–tactile interaction

The negative interaction contrast reveals somatosensory or tactile processing areas, where the activation difference ($VT+ - VT-$) decreases with increasing blur levels. While no activations were identified when correcting for multiple comparisons within the entire brain, the right posterior fusiform as one of our regions of interest showed a significant negative interaction (see Table 1). More specifically, the posterior fusiform showed increased activation for visuotactile (relative to visual conditions) when the visual stimulus is reliable. However, when the visual stimulus is completely blurred and unreliable, a concurrent tactile input suppresses and down weights visual induced activations.

To exclude the possibility that the observed results are confounded by differences in accuracy across the visual shape information conditions (higher proportion of incorrect responses at blur∞), we repeated the analysis on correct trials only. This additional analysis provided nearly equivalent results. In particular, it confirmed the interaction of visual and tactile processes bilaterally in the postcentral

A Visual-tactile interaction (positive)

bilateral postcentral sulcus (BA2)
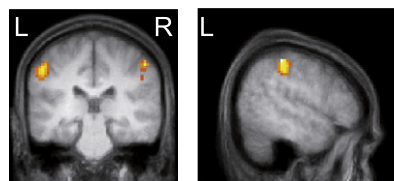
y = -29   x = -51

overlap with tactile processing areas
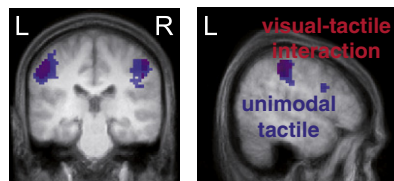
y = -29   x = -51

B Overlay on a cytoarchitectonic map
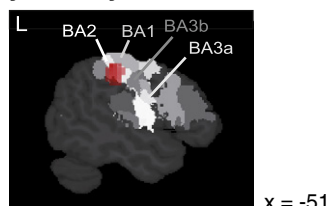
x = -51

C Visual-tactile interaction (negative)

right posterior fusiform gyrus
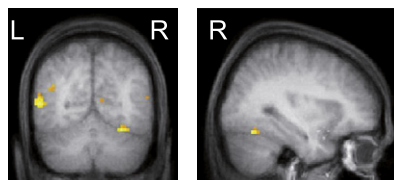
y = -63   x = 33

Fig. 3. Functional imaging results. A: Positive visual–tactile interaction in the left and right postcentral sulcus displayed on coronal and sagittal slices of a mean structural image created by averaging the subjects' normalized structural images. Height threshold: p<0.05 whole brain corrected at the cluster level. Lower panel: Overlap of tactile shape selective responses (blue) and visual–tactile interactions (red). B: The functional activation is overlaid on a probabilistic cytoarchitectonic map (maximum probability map, MPM) from the SPM Anatomy toolbox (Eickhoff et al., 2005). The activation peaks in the right and left postcentral sulci are assigned to area BA2 with a probability of 70%. C: Negative visual–tactile interaction in the right posterior fusiform displayed on coronal and sagittal slices of a mean structural image. Height threshold: p<0.001 uncorrected. (For interpretation of the references to color in this figure legend, the reader is referred to the web version of this article.)

sulcus (area 2) indicating that our interaction effects are less likely to be caused by differences in error related processes etc.

Summary of results

To summarize, we observed a positive visual–tactile interaction bilaterally in the postcentral sulci (area 2) and the left superior parietal lobe. All of these regions showed increased activation for tactile shape processing, when the reliability of visual shape information was reduced and hence, higher weight was attributed to the tactile modality.

At a lower threshold of significance, we also observed a negative i.e. opposite interaction in the right posterior fusiform where tactile input suppresses visual activations primarily when the visual input is completely blurred.

Discussion

The present fMRI study characterizes the neural basis of visual–tactile shape integration. We demonstrated that neural processing in somatosensory and visual areas was modulated in accordance with the relative reliabilities of the visual and tactile shape inputs.

Tactile shape processing was modulated by the reliability of visual shape information primarily at two levels within the somatosensory processing hierarchy, within the postcentral sulci bilaterally and the left superior parietal gyrus extending into the intraparietal sulcus.

The superior parietal gyrus (e.g., Kitada et al., 2006) and intraparietal sulcus (e.g., Grefkes et al., 2002) have previously been implicated in visual–tactile integration using conjunction analyses. These more posterior parietal areas showed shape-selective responses for both, visual and tactile modalities. Thus, visual and tactile information may converge in these regions and form higher order supramodal shape representations within a common spatial reference frame.

Our interaction design identified additional candidate regions for visual–tactile integration within the postcentral sulci, most likely Brodmann Area (BA) 2 within the primary somatosensory cortex. Previous functional imaging studies have implicated BA 2 predominantly in tactile shape processing: While BA 3b and 1 were equally activated for all kinds of mechanoreceptive stimulation, BA2 was the first region in the somatosensory processing hierarchy that was more activated for curvatures, edges, shape primitives and orientation discrimination (Kitada et al., 2006; van Boven et al., 2005; Bodegård et al., 2001; see also Randolph and Semmes, 1974; Koch and Fuster, 1989; Zhang et al., 2005). Interestingly, in line with previous studies of orientation judgments (Kitada et al., 2006), the interaction effects were observed not only in the contralateral but in both hemispheres (for related findings see also Iwamura et al., 1994) suggesting that higher order orientation and simple shape perception are represented bilaterally.

Our results extend these findings by demonstrating that activation in area 2 is not only evoked by tactile shape processing, but also modulated by the reliability of visual shape information. Increased activation for visual–tactile relative to visual shape processing was observed when the visual input was least reliable. These visual–tactile interactions suggest that even primary somatosensory cortices are involved in multisensory integration. They extend previous observations that somatosensory cortices activate not only for tactile but also for visual stimuli when presented alone (see Stilla and Sathian, 2008; Zhou and Fuster, 1997). However, in addition to interpreting our findings as evidence for multisensory interactions, two alternative mechanisms may also be discussed. First, one may argue that the activation increase in BA 2 is due to participants applying stronger forces when discriminating visual–tactile shapes in the context of unreliable visual information. Although we cannot fully exclude this possibility, as the applied forces were not measured online, this explanation seems unlikely. First, subjects were instructed and carefully trained to apply equal forces to all stimuli. Second, it would be rather surprising that increased "somatosensory" processing is only reflected at higher processing levels like BA2, yet we did not find any increased activations in BA3b. Second, one may invoke attentional shifts between visual and tactile modalities as an explanatory mechanism: unreliable visual shape information may have led subjects to attend more to tactile shape information. In this case, visual–tactile integration may perhaps in part be mediated by attentional shifts that were weighted by sensory reliability. Indeed, previous EEG and fMRI studies have demonstrated pronounced effects of attentional modulation in primary somatosensory cortex (Bauer et al., 2006; Burton et al., 1999; Macaluso et al., 2002; Noppeney et al., 1999). The current study cannot fully dissociate "genuine visual–tactile integration" from endogenous attentional shifts that are weighted according to the relative reliabilities of the two modalities. A future study using a dual task paradigm may help us to further disentangle these two explanatory
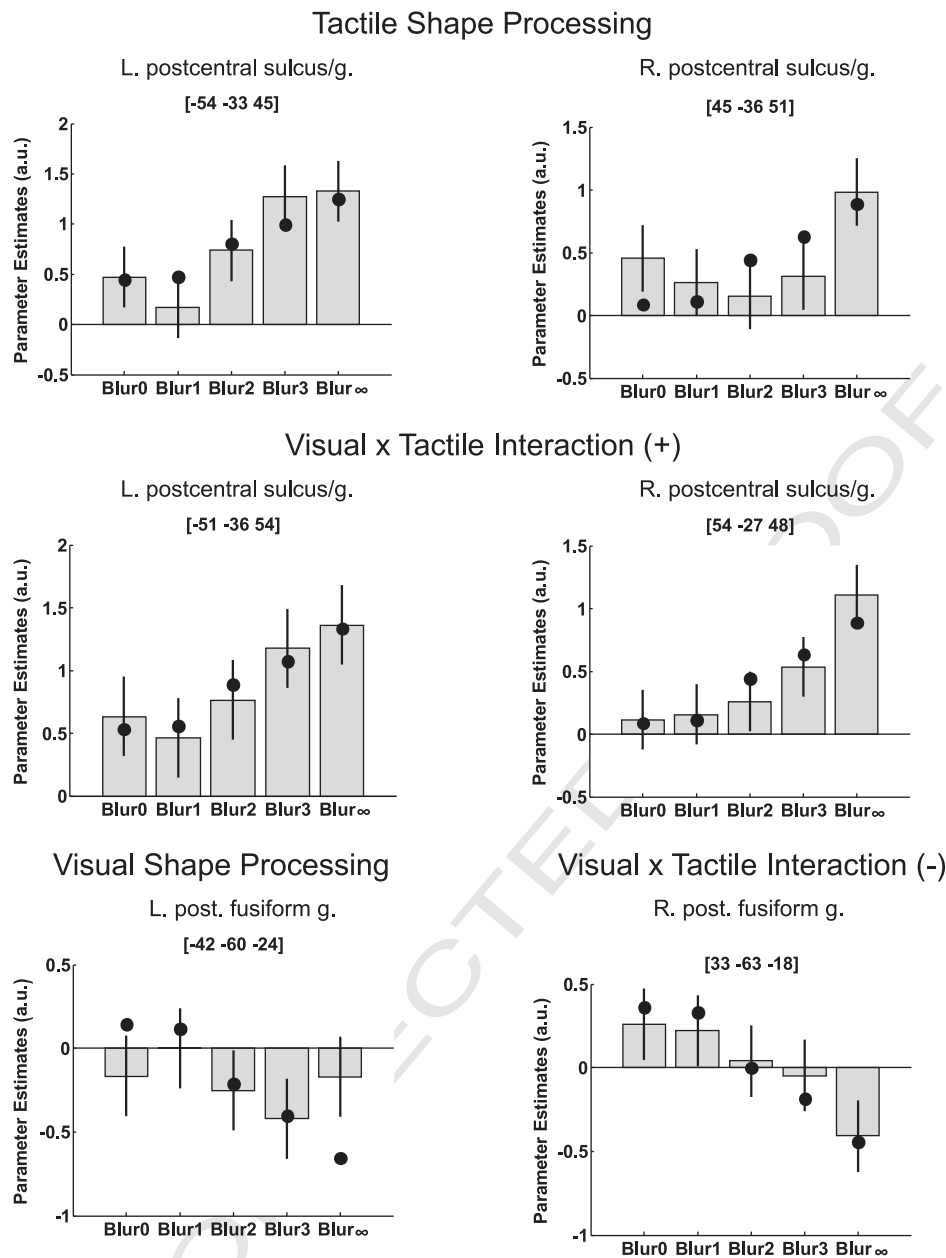
Fig. 4. Parameter estimates for the contrast Vblur(i)T+ − Vblur(i)T− (visual–tactile shape information versus visual shape alone) at the 5 levels of visual shape reliability (Vblur0, Vblur1, Vblur2, Vblur3, Vblur∞) at the given coordinates identified via the following statistical comparisons: Row 1: Tactile shape processing $(V_{blur\infty}T+) - (V_{blur\infty}T-)$. Row 2 : Positive visual–tactile interaction. Row 3 left : Visual shape processing $(V_{blur0}T-) - (V_{blur\infty}T-)$; Row 3 right : Negative visual–tactile interaction. The vertical bars represent the 90% confidence intervals. Black dots represent the positive (rows 1 + 2) or negative (row 3) tactile cue weights as derived from psychophysics based on the Maximum Likelihood Estimation model (Helbig and Ernst, 2007a). L = left, R = right.

mechanisms. In support of a more automatic visual–tactile integration mechanism, psychophysics data using a dual task paradigm failed to show significant effects of modality-specific attention on the weighting of sensory estimates during visual–haptic shape perception (Helbig and Ernst, 2008). Further, previous studies combining functional imaging and effective connectivity analyses have demonstrated that sensory reliability modulates the effective connectivity between sensory and higher order association areas, even when reliability changes rapidly over trials (Nath and Beauchamp, 2011; Noppeney et al., 2010). Yet, the role of endogenous and exogenous attention in reliability weighted multisensory integration is still relatively unexplored. In fact, even if reliability-weighting in multisensory integration is mediated by attentional shifts, our psychophysics and functional imaging results suggest that these shifts are optimal in the sense that they provide a visual–tactile percept that is more reliable than each individual sensory estimate.

Hence, from this alternative perspective, our results elucidate how the brain weights sensory estimates optimally according to their reliability via attentional modulation.

In summary, our results suggest that regional responses to tactile shape processing are increased when the visual input is degraded and unreliable, which is consistent with the principle of statistically optimal integration. They are also in line with recent neurophysiological studies demonstrating that bimodal neurons in MSTd in macaque monkeys integrate vestibular and visual cues by weighted linear summation of the responses at the single neuron level where the weights depend on the reliability of the unisensory cues (Gu et al., 2008; Morgan et al., 2008).

Importantly, these visual–tactile interactions emerge at two levels of the somatosensory processing hierarchy: (i) the superior parietal gyrus that has previously been implicated in visual–tactile integration

as it processes both visual and tactile shape input and (ii) in BA2 within the primary somatosensory cortex. Future studies are needed to further characterize and dissociate the contributions of automatic visual–tactile integration and attentional top-down in reliability weighted visual–tactile processing.

Conversely, the LOC as our a priori region of interest showed a significant interaction between visual reliability and the presence/absence of tactile shape information. Yet, as predicted, this interaction followed the opposite profile to that observed in the postcentral sulcus. As shown in the parameter estimate plots of Fig. 4, activation in the right posterior fusiform was increased for visuotactile relative to visual stimulation when the visual signal was very reliable and strongly weighted in the visuotactile percept. When the visual signal was completely blurred and hence unreliable, a concurrent tactile stimulus suppressed visual processing. Hence, activations in visual and somatosensory areas are well described by a seesaw relationship (Werner and Noppeney, 2011). An increase in activation in the somatosensory areas induced a decrease in visual areas and vice versa.

Multiple neural mechanisms have been proposed to mediate visual–tactile interactions in primary somatosensory cortices and visual areas. In line with the classical model of multisensory integration, visual–tactile convergence may be deferred to higher order association areas such as the superior parietal gyrus that then exerts top-down modulation onto lower level primary somatosensory and visual areas via backwards connections (e.g., Deshpande et al., 2008; Macaluso and Driver, 2005; Peltier et al., 2007). However, more recent neurophysiology, neuroanatomy and human EEG studies have accumulated evidence that multisensory integration may emerge early in putatively unisensory areas (Ghazanfar and Schroeder, 2006; Kayser and Logothetis, 2007; Werner and Noppeney, 2010b) or even at the thalamic level (Musacchia and Schroeder, 2009). Within this framework of early feed-forward integration, visual areas may directly interact with and modulate tactile evoked shape processing in primary somatosensory cortices and vice versa. Indeed, combining fMRI and Granger Causality analyses, Deshpande et al. (2008, 2010) have recently shown that different tasks may flexibly employ different effective connectivity structures. For instance, connectivity between somatosensory cortices and LOC was employed during processing of novel shapes, while imagery and processing familiar shapes relies more on top down effects.

Future complementary EEG studies of the same paradigm may provide essential timing information to distinguish between feed-forward vs. feed-back models of visual–tactile integration. For instance, a recent EEG study (Lucan et al., 2010) focusing on tactile shape processing suggested that LOC may become engaged in tactile shape processing at 160 ms poststimulus. This raises the question whether visual inputs may modulate concurrent tactile inputs at a similar or different latency.

In conclusion, the activation elicited by tactile shape processing in the bilateral postcentral sulcus (BA2) and the left superior parietal sulcus was enhanced, when the reliability of visual shape information was reduced and hence, higher weight was assigned to the tactile modality. These results indicate that visual and tactile processing interacts in primary somatosensory cortices and processing of tactile shape information is modulated by the reliability of the visual input. Conversely, tactile input suppressed activations and processing in the right posterior fusiform gyrus when the visual signal was unreliable. The modulatory effects on somatosensory and visual processing areas may be mediated either via direct connections from visual areas or top-down modulation from higher-order parietal association areas (for effective connectivity analyses see e.g., Deshpande et al., 2010; Lewis and Noppeney, 2010; Werner and Noppeney, 2010a, 2010b)

Uncited reference

Driver and Noesselt, 2008

References

Alais, D., Burr, D., 2004. The ventriloquist effect results from near-optimal bimodal integration. Curr. Biol. 14, 257–262.

Amedi, A., Malach, R., Hendler, T., Peled, S., Zohary, E., 2001. Visuo-haptic object-related activation in the ventral visual pathway. Nat. Neurosci. 4, 324–330.

Amedi, A., Jacobson, G., Hendler, T., Malach, R., Zohary, E., 2002. Convergence of visual and tactile shape processing in the human lateral occipital complex. Cereb. Cortex 12, 1202–1212.

Amedi, A., von Kriegstein, K., van Atteveldt, N.M., Beauchamp, M.S., Naumer, M.J., 2005. Functional imaging of human crossmodal identification and object recognition. Exp. Brain Res. 166, 559–571.

Avillac, M., Ben Hamed, S., Duhamel, J.R., 2007. Multisensory integration in the ventral intraparietal area of the macaque monkey. J. Neurosci. 27, 1922–1932.

Banati, R.B., Goerres, G.W., Tjoa, C., Aggleton, J.P., Grasby, P., 2000. The functional anatomy of visual–tactile integration in man: a study using positron emission tomography. Neuropsychologia 38, 115–124.

Barraclough, N.E., Xiao, D.K., Baker, C.I., Oram, M.W., Perrett, D.I., 2005. Integration of visual and auditory information by superior temporal sulcus neurons responsive to the sight of actions. J. Cogn. Neurosci. 17, 377–391.

Bauer, M., Oostenveld, R., Peeters, M., Fries, P., 2006. Tactile spatial attention enhances gamma-band activity in somatosensory cortex and reduces low-frequency activity in parieto-occipital areas. J. Neurosci. 26, 490–501.

Beauchamp, M.S., Argall, B.D., Bodurka, J., Duyn, J.H., Martin, A., 2004. Unraveling multisensory integration: patchy organization within human STS multisensory cortex. Nat. Neurosci. 7, 1190–1192.

Beauchamp, M.S., Pasalar, S., Ro, T., 2010. Neural substrates of reliability-weighted visual–tactile multisensory integration. Front. Syst. Neurosci. 4, 1–11 (Article 25).

Bodegård, A., Geyer, S., Grefkes, C., Zilles, K., Roland, P.E., 2001. Hierarchical processing of tactile shape in the human brain. Neuron 31, 317–328.

Bonath, B., Noesselt, T., Martinez, A., Mishra, J., Schwiecker, K., Heinze, H.J., Hillyard, S.A., 2007. Neural basis of the ventriloquist illusion. Curr. Biol. 17, 1697–1703.

Burton, H., Abend, N.S., MacLeod, A.M., Sinclair, R.J., Snyder, A.Z., Raichle, M.E., 1999. Tactile attention tasks enhance activation in somatosensory regions of parietal cortex: a positron emission tomography study. Cereb. Cortex 9, 662–674.

Calvert, G.A., Hansen, P.C., Iversen, S.D., Brammer, M.J., 2001. Detection of audio–visual integration sites in humans by application of electrophysiological criteria to the BOLD effect. Neuroimage 14, 427–438.

Deshpande, G., Hu, X., Stilla, R., Sathian, K., 2008. Effective connectivity during haptic perception: a study using Granger causality analysis of functional magnetic resonance imaging data. Neuroimage 40, 1807–1814.

Deshpande, G., Hu, X., Lacey, S., Stilla, R., Sathian, K., 2010. Object familiarity modulates effective connectivity during haptic shape perception. Neuroimage 49, 1991–2000.

Driver, J., Noesselt, T., 2008. Multisensory interplay reveals crossmodal influences on 'sensory-specific' brain regions, neural responses, and judgments. Neuron 57, 11–23.

Eickhoff, S.B., Stephan, K.E., Mohlberg, H., Grefkes, C., Fink, G.R., Amunts, K., Zilles, K., 2005. A new spm toolbox for combining probabilistic cytoarchitectonic maps and functional imaging data. Neuroimage 25, 1325–1335.

Ernst, M.O., Banks, M.S., 2002. Humans integrate visual and haptic information in a statistically optimal fashion. Nature 415, 429–433.

Ernst, M.O., Bülthoff, H.H., 2004. Merging the senses into a robust percept. Trends Cogn. Neurosci. 8, 162–169.

Evans, A.C., Marrett, S., Neelin, P., Collins, L., Worsley, K., Dai, W., Milot, S., Meyer, E., Bub, D., 1992. Anatomical mapping of functional activation in stereotactic coordinate space. Neuroimage 1, 43–53.

Foxe, J.J., Schroeder, C.E., 2005. The case for feedforward multisensory convergence during early cortical processing. Neuroreport 16, 419–423.

Friston, K.J., Holmes, A.P., Worsley, K.J., 1999. How many subjects constitute a study? Neuroimage 10, 1–5.

Gentile, G., Petkova, V.I., Ehrsson, H.H., 2011. Integration of visual and tactile signals from the hand in the human brain: an FMRI study. J. Neurophysiol. 105, 910–922.

Ghazanfar, A.A., Schroeder, C.E., 2006. Is neocortex essentially multisensory? Trends Cogn. Sci. 10, 278–285.

Ghazanfar, A.A., Maier, J.X., Hoffman, K.L., Logothetis, N.K., 2005. Multisensory integration of dynamic faces and voices in rhesus monkey auditory cortex. J. Neurosci. 25, 5004–5012.

Ghazanfar, A.A., Chandrasekaran, C., Logothetis, N.K., 2008. Interactions between the superior temporal sulcus and auditory cortex mediate dynamic face/voice integration in rhesus monkeys. J. Neurosci. 28, 4457–4469.

Grefkes, C., Weiss, P.H., Zilles, K., Fink, G.R., 2002. Crossmodal processing of object features in human anterior intraparietal cortex: an fMRI study implies equivalencies between humans and monkeys. Neuron 35, 173–184.

Grill-Spector, K., Kushnir, T., Edelman, S., Avidan, G., Itzchak, Y., Malach, R., 1999. Differential processing of objects under various viewing conditions in the human lateral occipital complex. Neuron 24, 187–203.

Gu, Y.A., Angelaki, D.E., DeAngelis, G.C., 2008. Neural correlates of multisensory cue integration in macaque MSTd. Nat. Neurosci. 11, 1201–1210.

Hadjikhani, N., Roland, P.E., 1998. Cross-modal transfer of information between the tactile and the visual representations in the human brain: a positron emission tomographic study. J. Neurosci. 18, 1072–1084.

Helbig, H.B., Ernst, M.O., 2007a. Optimal integration of shape information from vision and touch. Exp. Brain Res. 179, 595–606.

Helbig, H.B., Ernst, M.O., 2007b. Knowledge about a common source can promote visual haptic integration. Perception 36, 1523–1533.

Helbig, H.B., Ernst, M.O., 2008. Visual–haptic cue weighting is independent of modality-specific attention. J. Vis. 8 (21), 1–16.

Hillis, J.M., Watt, S.J., Landy, M.S., Banks, M.S., 2004. Slant from texture and disparity cues: optimal cue combination. J. Vis. 4, 967–992.

Iwamura, Y., Iriki, A., Tanaka, M., 1994. Bilateral hand representation in the postcentral somatosensory cortex. Nature 369 (6481), 554–556.

James, T.W., Humphrey, G.K., Gati, J.S., Servos, P., Menon, R.S., Goodale, M.A., 2002. Haptic study of three-dimensional objects activates extrastriate visual areas. Neuropsychologia 40, 1706–1714.

Kayser, C., Logothetis, N.K., 2007. Do early sensory cortices integrate cross-modal information? Brain Struct. Funct. 212, 121–132.

Kayser, C., Petkov, C.I., Augath, M., Logothetis, N.K., 2005. Integration of touch and sound in auditory cortex. Neuron 48, 373–384.

Kayser, C., Petkov, C.I., Augath, M., Logothetis, N.K., 2007. Functional imaging reveals visual modulation of specific fields in auditory cortex. J. Neurosci. 27, 1824–1835.

Kayser, C., Petkov, C.I., Logothetis, N.K., 2008. Visual modulation of neurons in auditory cortex. Cereb. Cortex 18, 1560–1574.

Kim, S., James, T.W., 2010. Enhanced effectiveness in visuo-haptic object-selective brain regions with increasing stimulus salience. Hum. Brain Mapp. 31, 678–693.

Kitada, R., Kito, T., Saito, D.N., Kochiyama, T., Matsumura, M., Sadato, N., Lederman, S.J., 2006. Multisensory activation of the intraparietal area when classifying grating orientation: a functional magnetic resonance imaging study. J. Neurosci. 26, 7491–7501.

Knill, D.C., Saunders, J.A., 2003. Do humans optimally integrate stereo and texture information for judgments of surface slant? Vis. Res. 43, 2539–2558.

Koch, K.W., Fuster, J.M., 1989. Unit activity in monkey parietal cortex related to haptic perception and temporary memory. Exp. Brain Res. 76, 292–306.

Lakatos, P., Chen, C.M., O'Connell, M.N., Mills, A., Schroeder, C.E., 2007. Neuronal oscillations and multisensory interaction in primary auditory cortex. Neuron 53, 279–292.

Lewis, R., Noppeney, U., 2010. Audiovisual synchrony improves motion discrimination via enhanced connectivity between early visual and auditory areas. J. Neurosci. 30, 12329–12339.

Lucan, J.N., Foxe, J.J., Gomez-Ramirez, M., Sathian, K., Molholm, S., 2010. Tactile shape discrimination recruits human lateral occipital complex during early perceptual processing. Hum. Brain Mapp. 31, 1813–1821.

Macaluso, E., Driver, J., 2005. Multisensory spatial interactions: a window onto functional integration in the human brain. Trends Neurosci. 28, 264–271.

Macaluso, E., Frith, C.D., Driver, J., 2002. Directing attention to locations and to sensory modalities: multiple levels of selective processing revealed with PET. Cereb. Cortex 12, 357–368.

Macaluso, E., Driver, J., Frith, C.D., 2003. Multimodal spatial representations engaged in human parietal cortex during both saccadic and manual spatial orienting. Curr. Biol. 13, 990–999.

Malach, R., Reppas, J.B., Benson, R.R., Kwong, K.K., Jiang, H., Kennedy, W.A., Ledden, P.J., Brady, T.J., Rosen, B.R., Tootell, R.B., 1995. Object-related activity revealed by functional magnetic resonance imaging in human occipital cortex. Proc. Natl. Acad. Sci. U.S.A. 92, 8135–8139.

Martuzzi, R., Murray, M.M., Michel, C.M., Thiran, J.P., Maeder, P.P., Clarke, S., Meuli, R.A., 2007. Multisensory interactions within human primary cortices revealed by BOLD dynamics. Cereb. Cortex 17, 1672–1679.

Miller, L.M., D'Esposito, M., 2005. Perceptual fusion and stimulus coincidence in the cross-modal integration of speech. J. Neurosci. 25, 5884–5893.

Molholm, S., Ritter, W., Javitt, D.C., Foxe, J.J., 2004. Multisensory visualauditory object recognition in humans: a high-density electrical mapping study. Cereb. Cortex 14, 452–465.

Morgan, M.L., DeAngelis, G.C., Angelaki, D.E., 2008. Multisensory integration in macaque visual cortex depends on cue reliability. Neuron 59, 662–673.

Musacchia, G., Schroeder, C.E., 2009. Neuronal mechanisms, response dynamics and perceptual functions of multisensory interactions in auditory cortex. Hear. Res. 258, 72–79.

Nath, A.R., Beauchamp, M.S., 2011. Dynamic changes in superior temporal sulcus connectivity during perception of noisy audiovisual speech. J. Neurosci. 31, 1704–1714.

Noesselt, T., Rieger, J.W., Schoenfeld, M.A., Kanowski, M., Hinrichs, H., Heinze, H.J., Driver, J., 2007. Audiovisual temporal correspondence modulates human multisensory superior temporal sulcus plus primary sensory cortices. J. Neurosci. 27, 11431–11441.

Noppeney, U., 2011. Characterization of multisensory integration with fMRI: experimental design, statistical analysis and interpretation. In: Murray, M.M., Wallace, M.T. (Eds.), Frontiers in the Neural Basis of Multisensory Processes. CRC Press, Boca Raton, FL, USA.

Noppeney, U., Waberski, T.D., Gobbelé, R., Buchner, H., 1999. Spatial attention modulates the cortical somatosensory representation of the digits in humans. Neuroreport 10, 3137–3141.

Noppeney, U., Josephs, O., Hocking, J., Price, C.J., Friston, K.J., 2008. The effect of prior visual information on recognition of speech and sounds. Cereb. Cortex 18, 598–609.

Noppeney, U., Ostwald, D., Werner, S., 2010. Perceptual decisions formed by accumulation of audiovisual evidence in prefrontal cortex. J. Neurosci. 30, 7434–7446.

Peltier, S., Stilla, R., Mariola, E., LaConte, S., Hu, X., Sathian, K., 2007. Activity and effective connectivity of parietal and occipital cortical regions during haptic shape perception. Neuropsychologia 45, 476–483.

Pietrini, P., Furey, M.L., Ricciardi, E., Gobbini, M.I., Wu, W.H.C., Cohen, L., Guazzelli, M., Haxby, J.V., 2004. Beyond sensory images: object-based representation in the human ventral pathway. Proc. Natl. Acad. Sci. U.S.A. 101, 5658–5663.

Prather, S.C., Votaw, J.R., Sathian, K., 2004. Task-specific recruitment of dorsal and ventral visual areas during tactile perception. Neuropsychologia 42, 1079–1087.

Randolph, M., Semmes, J., 1974. Behavioral consequences of selective subtotal ablations in the postcentral gyrus of Macaca mulatta. Brain Res. 70, 55–70.

Sadaghiani, S., Maier, J.X., Noppeney, U., 2009. Natural, metaphoric, and linguistic auditory direction signals have distinct influences on visual motion processing. J. Neurosci. 29, 6490–6499.

Saito, D.N., Okada, T., Morita, Y., Yonekura, Y., Sadato, N., 2003. Tactile–visual cross-modal shape matching: a functional MRI study. Cogn. Brain Res. 17, 14–25.

Schroeder, C.E., Foxe, J.J., 2002. The timing and laminar profile of converging inputs to multisensory areas of the macaque neocortex. Brain Res. Cogn. Brain Res. 14, 187–198.

Stilla, R., Sathian, K., 2008. Selective visuo-haptic processing of shape and texture. Hum. Brain Mapp. 29, 1123–1138.

Stoesz, M.R., Zhang, M., Weisser, V.D., Prather, S.C., Mao, H., Sathian, K., 2003. Neural networks active during tactile form perception: common and differential activity during macrospatial and microspatial tasks. Int. J. Psychophysiol. 50 (1–2), 41–49.

Tal, N., Amedi, A., 2008. Using fMR-adaptation to study visual–tactile integration of objects in humans. Abstract, Israel Society for Neuroscience. .

Treisman, M., 1998. Combining information: probability summation and probability averaging in detection and discrimination. Psychol. Methods 3, 252–265.

Van Atteveldt, N., Formisano, E., Goebel, R., Blomert, L., 2004. Integration of letters and speech sounds in the human brain. Neuron 43, 271–282.

Van Boven, R.W., Ingeholm, J.E., Beauchamp, M.S., Bikle, P.C., Ungerleider, L.G., 2005. Tactile form and location processing in the human brain. Proc. Natl. Acad. Sci. U.S.A. 102, 12601–12605.

Vinberg, J., Grill-Spector, K., 2008. Representation of shapes, edges, and surfaces across multiple cues in the human visual cortex. J. Neurophysiol. 99, 1380–1393.

Wallace, M.T., Wilkinson, L.K., Stein, B.E., 1996. Representation and integration of multiple sensory inputs in primate superior colliculus. J. Neurophysiol. 76, 1246–1266.

Werner, S., Noppeney, U., 2010a. Superadditive responses in superior temporal sulcus predict audiovisual benefits in object categorization. Cereb. Cortex 20, 1829–1842.

Werner, S., Noppeney, U., 2010b. Distinct functional contributions of primary sensory and association areas to audiovisual integration in object categorization. J. Neurosci. 30, 2662–2675.

Werner, S., Noppeney, U., 2011. The contributions of transient and sustained response codes to audiovisual integration. Cereb. Cortex 21, 920–931.

Zhang, M., Weisser, V.D., Stilla, R., Prather, S.C., Sathian, K., 2004. Multisensory cortical processing of object shape and its relation to mental imagery. Cogn. Affect. Behav. Neurosci. 4, 251–259.

Zhang, M., Mariola, E., Stilla, R., Stoesz, M., Mao, H., Hu, X., Sathian, K., 2005. Tactile discrimination of grating orientation: fMRI activation patterns. Hum. Brain Mapp. 25, 370–377.

Zhou, Y.D., Fuster, J.M., 1997. Neuronal activity of somatosensory cortex in a cross-modal (visuo-haptic) memory task. Exp. Brain Res. 116, 551–555.